



## High cycle torsional fatigue properties of 17-4PH stainless steel

K. Yanase

*Fukuoka University*

*kyanase@fukuoka-u.ac.jp, http://www.fukuoka-u.ac.jp/english/*

B.M. Schönauer

*University of Natural Resources and Life Sciences (BOKU)*

*bernd.schoenbauer@boku.ac.at, https://www.boku.ac.at/en/*

M. Endo

*Fukuoka University*

*endo@fukuoka-u.ac.jp, http://www.fukuoka-u.ac.jp/english/*

**ABSTRACT.** Sensitivity to small defects under torsional fatigue loading condition is examined in the high cycle fatigue regime. Fatigue crack initiation and small crack growth behaviors were observed during fatigue testing and fractographic investigations were performed. The results are compared to the data obtained in the uniaxial fatigue tests, which allows the effect of biaxial stresses on the surface of material to be discussed. Finally, an approach for predicting the fatigue limit of 17-4PH stainless steel under torsional and tension-compression fatigue loadings is presented.

**KEYWORDS.** 17-4PH; Small defect; Torsion; Biaxial fatigue; Fatigue limit.

### INTRODUCTION

Precipitation-hardened chromium-nickel-copper stainless steel 17-4PH possesses high strength, toughness and good corrosion resistance. Therefore, it is widely used in applications where good corrosion resistance as well as high strength are required, e.g., in the aerospace, chemical, food processing, paper and power industry. In the last few decades, a number of investigations on the uniaxial fatigue properties of 17-4PH have been performed; however, no results of torsional fatigue tests are presently available. In practice, there are several applications for the material in which components (e.g., bearing outer rings, propeller shafts and pressure safety valve springs) are exposed to torsional fatigue loading and where a high number of load cycles is accumulated within service life. Given the substantial knowledge on uniaxial fatigue, it is of practical merit to propose a predictive method that can connect the fatigue strength under multiaxial loading with that under uniaxial loading.

In our previous studies [1,2], a series of tension-compression fatigue tests were carried out to elucidate the uniaxial fatigue properties of 17-4PH stainless steel in the high and very high cycle fatigue regimes. It was found that the material exhibits interesting properties that are different from those noted for conventional steels. For example, the defect tolerance under cyclic loading is highly dependent on the notch root radius, which makes the prediction of the fatigue strength in the presence of small flaws challenging.



As an extension of our previous work [1,2], further fatigue tests under torsional loading at  $R = -1$  were conducted and the results yielded are reported in this paper. In particular, material sensitivity to small defects under torsional fatigue loading condition is examined in the high cycle fatigue regime. Furthermore, fatigue crack initiation and small crack growth behavior were observed during fatigue testing and fractographic investigations were performed. The results are compared to the data obtained in the tension-compression fatigue tests and the effects of biaxial stresses on the surface of material are discussed. Finally, the experimental data are evaluated to examine the predictive approach (cf. [3-7]) for the fatigue strength of 17-4PH stainless steel under torsional and tension-compression fatigue loadings.

## MATERIAL AND EXPERIMENT

The testing material used in the present investigation was a chromium-nickel-copper stainless steel 17-4PH precipitation hardened at 913 °C and age hardened at 621 °C for 4 h (condition H1150). The material properties at room temperature are summarized in Tab. 1, and the average grain size is 11 µm (independent of orientation). For more details, we refer to Schönauer et al. [1].

The surface of a round-bar specimen was ground and electropolished to remove the residual stress. Artificial defects (one-hole, two-hole, and three-hole, respectively) were introduced in the gage length of the specimen (length = 10 mm, Fig. 1). The major axes of two-hole and three-hole defects were intentionally set to be perpendicular to the direction of the major principal stress. To remove any residual stresses that were possibly generated during drilling, the specimens were stress-relief annealed in a vacuum at 600°C for one hour. Fatigue tests were performed by using a servohydraulic testing machine at stress ratio  $R = -1$ .

Tensile strength (MPa)	Yield strength (MPa)	Elongation (%)	Reduction of area (%)	Vickers hardness (kgf/mm <sup>2</sup> )
1030	983	21	61	352

Table 1: Mechanical properties of the 17-4PH at room temperature.

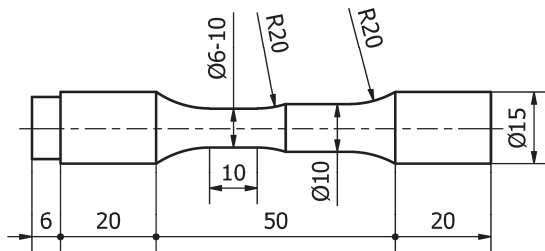


Figure 1: Specimen shape and geometry for the torsional fatigue test.

## RESULTS AND DISCUSSION

In this section, the obtained experimental data are examined by considering the effects of the principal stresses on the surface of specimen and  $\sqrt{area}$  [8]. Here,  $\sqrt{area}$  is defined as the square root of the projection area perpendicular to the major principal stress direction. Furthermore, the characteristic properties of 17-4PH stainless steel are discussed.

### Fatigue Crack Growth Behavior

Concerning the one-hole defect (diameter = 100 µm, depth = 63 µm,  $\sqrt{area} = 70$  µm), all specimens failed from smooth part rather than originating from the hole. Accordingly, this defect had no influence on the fatigue limit. However, small mixed mode cracks (Mode III and I) were observed at the bottom and at the edge of the hole, respectively, as shown in Fig. 2. Examination of the specimens with the two-hole defect (diameter = 2×100 µm, depth = 131 µm,  $\sqrt{area} = 161$  µm) and the three-hole defect (diameter = 3×100 µm, depth = 280 µm,  $\sqrt{area} = 274$  µm) showed that failure originated from

holes associated with Mode I fatigue crack growth in the principal stress direction (i.e., 45 degrees from the specimen axis), as shown in Fig. 3.

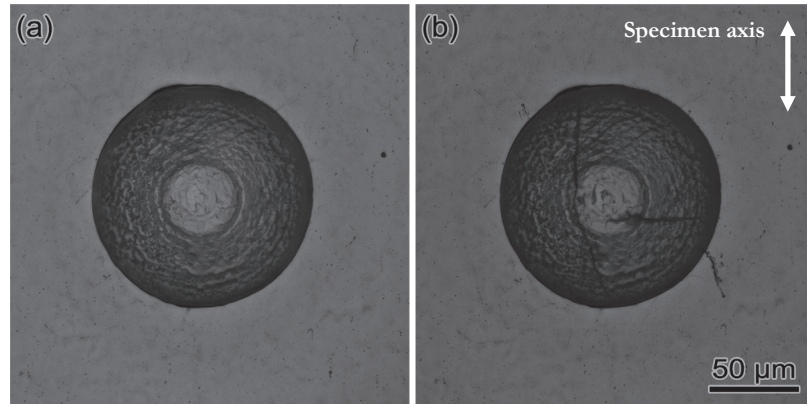


Figure 2: One-hole defect (a) before and (b) after fatigue testing at shear stress amplitude,  $\tau_a = 320$  MPa and number of cycles,  $N = 2.8 \times 10^7$  cycles.

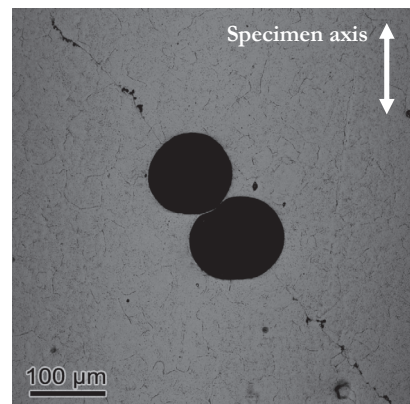


Figure 3: Mode I fatigue crack growth from a two-hole defect under torsional loading at shear stress amplitude,  $\tau_a = 290$  MPa.

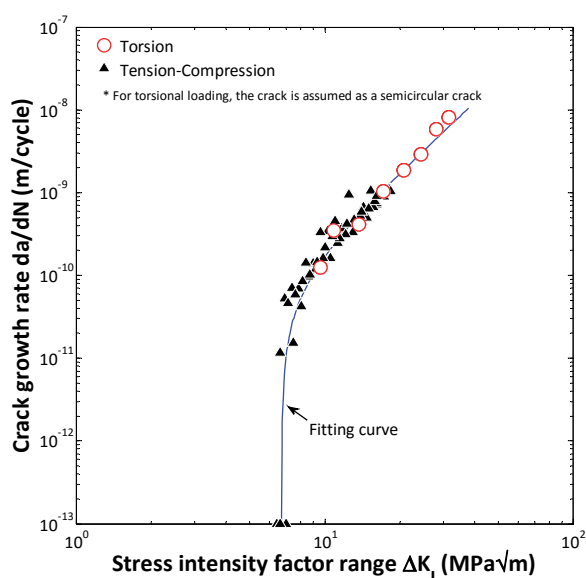


Figure 4: FCGR curves for Mode I crack under torsional loading and tension-compression loading [9].



In Fig. 4, the fatigue crack growth rate (FCGR) under torsional loading is compared to that under tension-compression loading [9]. It is noted that, for torsional loading, the stress intensity factor range is calculated by assuming a semi-circular crack. As shown, FCGR can be uniquely characterized irrespective of the difference of loading condition. However, the crack shape is not necessarily semi-circular, as was noted for a medium carbon steel (JIS S35C) (Fig. 5, [10]). Accordingly, a further study is necessary to inspect the evolution of crack shape and its effect on the torsional fatigue behavior of 17-4PH.

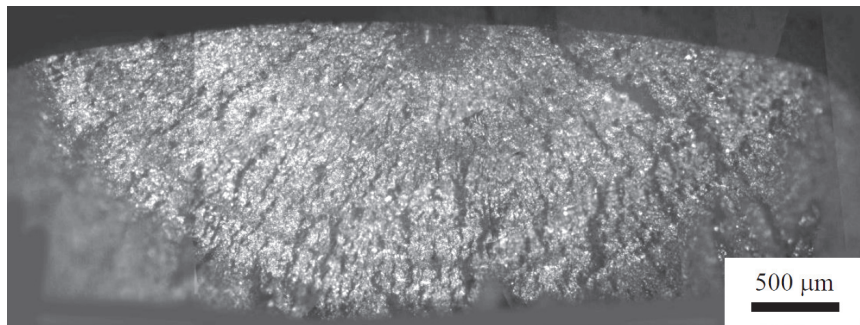


Figure 5: Crack profile propagating from an artificial defect in a medium carbon steel (JIS S35C) under torsional loading ( $R = -1$ ) [10].

#### Fatigue Limit

By considering the major principal stress  $\sigma_1$  and the minor principal stress  $\sigma_2$  on the surface of material, the fatigue limit can be expressed as [3]:

$$\begin{aligned} \sigma_1 + k\sigma_2 &= \sigma_w \\ &= \frac{1.43(HV + 120)}{(\sqrt{\text{area}})^{1/6}} \end{aligned} \quad (1)$$

where  $HV$  signifies the Vickers hardness. Under torsional loading, the principal stresses are rendered as  $\sigma_1 = \tau$  and  $\sigma_2 = -\tau$  (Fig. 6). Therefore, Eq. (1) can be rewritten to yield:

$$(1-k)\tau_w = \frac{1.43(HV + 120)}{(\sqrt{\text{area}})^{1/6}} \rightarrow \tau_w = \left( \frac{1}{1-k} \right) \times \frac{1.43(HV + 120)}{(\sqrt{\text{area}})^{1/6}} \quad (2)$$

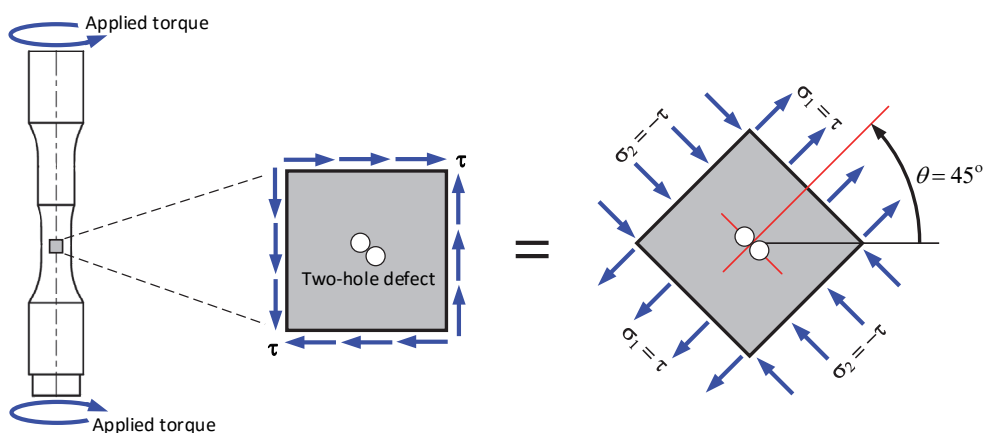


Figure 6: Stress transformation on the specimen surface (cf. Fig. 3).

According to the previously reported results [3-7],  $k = -0.18$  holds for carbon steels, Cr-Mo steel, ductile cast irons, and high tension brass. If the effect of biaxial stress is negligible (i.e.,  $k = 0$ ), the torsional fatigue limit is solely determined by the major principal stress as follows (cf. Fig. 6):

$$\tau_w = \frac{1.43(HV + 120)}{(\sqrt{area})^{1/6}} = \sigma_w \quad (3)$$

On the other hand, Schönbauer et al. proposed that the fatigue limit in the presence of a large defect or a long crack can be estimated by the following equation [2]:

$$\sigma_w = \frac{\Delta K_{th,lc}}{2 \times 0.65\sqrt{\pi}\sqrt{area}} \quad (4)$$

where the threshold stress intensity factor range of  $\Delta K_{th,lc} = 6.7 \text{ MPa}\sqrt{\text{m}}$  for the investigated 17-4PH steel at  $R = -1$  was determined by Schönbauer et al. [9].

Fig. 7 shows the relationship between the shear stress amplitude  $\tau_a$  and  $\sqrt{area}$ . When a specimen endured the number of cycles  $N = 1.2 \times 10^7$ , it was regarded as a run-out specimen. As shown, the prediction for fatigue limit with  $k = 0$  (Fig. 7(b)) renders higher correlation to the experimental data than using  $k = -0.18$  (Fig. 7(a)). Further, for the torsional loading, fatigue limit can be reasonably estimated by the two prediction lines:  $\tau_a = 0.6 \times (1.6HV)$  and the threshold for long crack (cf. Eq. (4)).

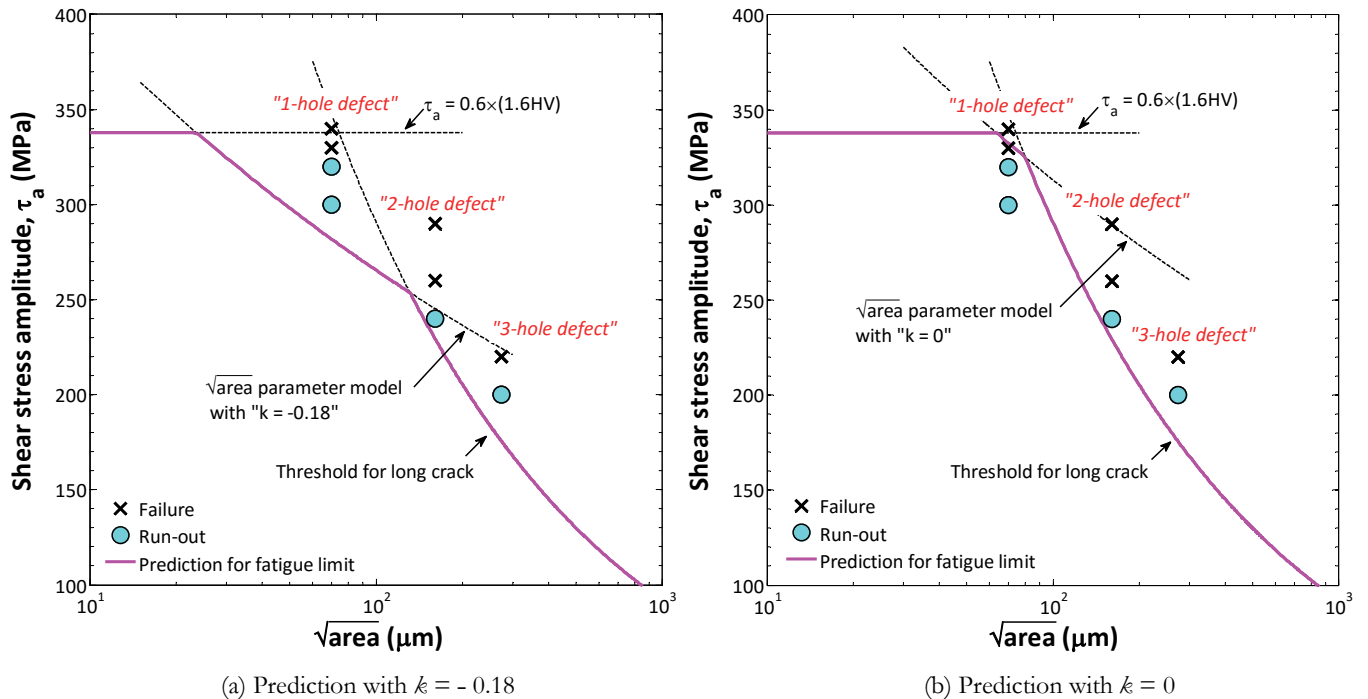


Figure 7: Relationship between shear stress amplitude  $\tau_a$  and  $\sqrt{area}$ .

In Fig. 8, fatigue limit for torsional loading and tension-compression loading is compared [2]. It is noted that, in the tension-compression data, various types of defects are considered (e.g., drilled hole, circumferential notch, corrosion pit). As shown, the respective fatigue limit can be reasonably estimated by considering the major principal stress (i.e.,  $k = 0$ ) and  $\sqrt{area}$ . The torsional fatigue limit becomes insensitive to the defect when  $\sqrt{area} < 100 \mu\text{m}$ , which is in strong contrast



to that for tension-compression loading. Concerning the tension-compression loading, the  $\sqrt{area}$  parameter model (cf. Eq. (3)) can be used for 17-4PH when  $\sqrt{area} < 100 \mu\text{m}$ , which is much less than  $\sqrt{area} < 1000 \mu\text{m}$  for the conventional carbon steels. Fig. 8 clearly shows that the aforementioned one-hole defect ( $\sqrt{area} = 70 \mu\text{m}$ ) has negligible influence on fatigue limit under torsional loading. Finally, as some experimental data significantly deviate from the prediction line, a further study is necessary to elucidate the reasons behind these discrepancies.

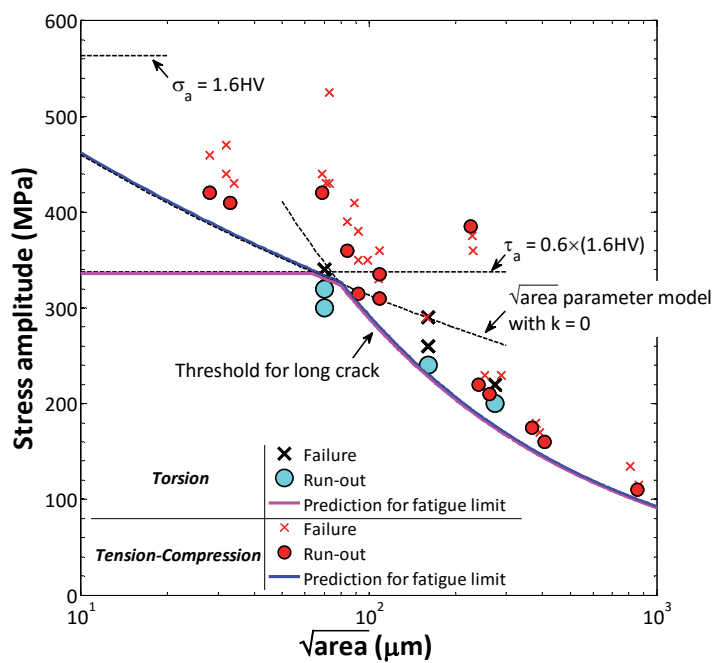


Figure 8: Relationship between stress amplitude and  $\sqrt{area}$ .

## CONCLUSIONS

In this study, the torsional fatigue behavior of precipitation-hardened chromium-nickel-copper stainless steel 17-4PH was investigated in the presence of small defects. It was shown that the dimensions of defects can be evaluated by the square root of the projection area perpendicular to the major principal stress direction,  $\sqrt{area}$ . The results pertaining to the fatigue crack growth behavior and fatigue limit demonstrate that the effect of biaxial stress on the surface of specimen is negligible and the major principal stress governs the fatigue behavior under torsional loading.

## REFERENCES

- [1] Schönbauer, B.M., Yanase, K. and Endo, M., VHCF properties and fatigue limit prediction of precipitation hardened 17-4PH stainless steel, *Int. J. Fatigue*, 88 (2016) 205-216. DOI: 10.1016/j.ijfatigue.2016.03.034.
- [2] Schönbauer, B.M., Yanase, K. and Endo, M., to be submitted to *Int. J. Fatigue*.
- [3] Endo, M. and Ishimoto, I., The fatigue strength of steels containing small holes under out-of-phase combined loading, *Int. J. Fatigue*, 28 (2006) 592-597. DOI: 10.1016/j.ijfatigue.2005.05.013.
- [4] Endo, M. and Ishimoto, I., *J. Solid Mech. Mater. Engng. (JSME)*, 1 (2007), 343-354, DOI: 10.1299/jmmp.1.343.
- [5] Yanase, K., A study on the multiaxial fatigue failure criterion with small defects, *ASTM Mater. Perform. Charact.*, 2 (2013) 1-9. DOI: 10.1520/MPC20130013.
- [6] Yanase K., Endo M., Multiaxial high cycle fatigue threshold with small defects and cracks, *Engng. Fract. Mech.*, 123 (2014) 182-196. DOI: 10.1016/j.engfracmech.2014.03.017.



- [7] Endo, M., Yanase, K., Effects of small defects, matrix structures and loading conditions on the fatigue strength of ductile cast irons, *Theor. Appl. Fract. Mech.*, 69 (2014) 34-43. DOI: 10.1016/j.tafmec.2013.12.005.
- [8] Murakami, Y., *Metal Fatigue: Effects of Small Defects and Nonmetallic Inclusions*, Elsevier, Oxford (2002), Chapter 4 – Effects of size and geometry of small defects on the fatigue limit. DOI: 10.1016/B978-008044064-4/50004-9.
- [9] Schönbauer, B.M., Stanzl-Tschegg, S.E., Perlega, A., Salzman R.N., Rieger, N.F., Turnbull, A., Zhou, S., Lukaszewicz, M., Gandy, D., The influence of corrosion pits on the fatigue life of 17-4PH steam turbine blade steel, *Engng. Fract. Mech.*, 147 (2015) 158-175. DOI: 10.1016/j.engfracmech.2015.08.011.
- [10] Ikeda, S. The effects of biaxial stress and stress gradient on fatigue crack growth behavior, Master Thesis (2008), Fukuoka University.